ACS APPLIED MATERIALS & INTERFACES

Research Article

www.acsami.org

Design of Antimicrobial Membrane Based on Polymer Colloids/Multiwall Carbon Nanotubes Hybrid Material with Silver Nanoparticles

Edina Rusen,[†] Alexandra Mocanu,[†] Leona Cristina Nistor,[‡] Adrian Dinescu,[§] Ioan Călinescu,[†] Gabriel Mustăţea,[†,∥] Ştefan Ioan Voicu,[⊥] Corina Andronescu,[†] and Aurel Diacon*[,†]

[†]Department of Bioresources and Polymer Science, University Politehnica of Bucharest, 149 Calea Victoriei, RO-010072 Bucharest, Romania

[‡]National Institute of Materials Physics, 105 bis Atomistilor, 077125 Magurele-Ilfov, Romania

[§]National Institute for Research and Development in Microtechnologies (IMT-Bucharest), 126 A, Erou Iancu Nicolae Street, 077190, PO-BOX 38-160, 023573 Bucharest, Romania

[∥]National Institute of Research and Development for Food Bioresources − IBA Bucharest, 5 Ancuta Baneasa, 020323 Bucharest 2, Romania

[⊥]Faculty of Applied Chemistry and Materials Science, University Politehnica of Bucharest, 1-7 Gh. Polizu Street, 011061 Bucharest, Romania

Supporting Information

ABSTRACT: The aim of this study was to obtain membranes with antimicrobial activity presenting a complex sandwich-type structure. The outer layers are comprised of poly(methyl methacrylate) membranes, whereas the inner active layer consists of a modified commercial membrane to achieve antimicrobial properties. This activity arises due to the presence of silver nanoparticles in a material with a hybrid composition deposited on a commercial membrane. This hybrid material consists of polymer colloids and multiwall carbon nanotubes used for both the stabilization of the active layer by the interconnections of the polymer particles and as active component. The filtration tests revealed a good stability of the materials and an increased hydrophilicity of the hybrid membranes. The antimicrobial properties have been evaluated using *Staphylococcus aureus* and *Escherichia coli*, and have been correlated with the content and migration rate of silver ions.

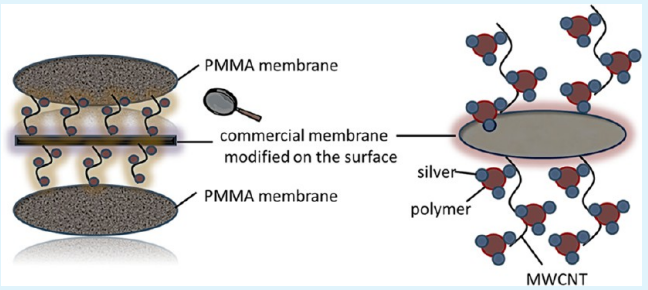

KEYWORDS: *membrane, antimicrobial, silver nanoparticles, multiwall carbon nanotubes, polymer colloids*

1. INTRODUCTION

Silver represents an important alternative for conferring antimicrobial properties to materials, being used in various domains.[1−7] The antimicrobial activity is dependent on the Ag particle dimensions, which represents one of the motivations in obtaining nanosized Ag particles.[7−9] Synthesis of Ag nanoparticles has been achieved by various routes consisting of complex synthesis/reduction procedures such as coprecipitation,[10] microemulsion,[11] sonochemical,[12,13] biosynthesis,[14] high-energy irradiation,[15] and chemical or photochemical techniques.[16] The aggregation of the nanoparticles in solution can be prevented by the use of stabilizing agents. One of the most widely used methods consists of adding to the solutions with long alkyl chain organic ligands bearing functional groups such as thiols,[17] carboxilates,[18] poly(vinyl alcohol)s, poly(ethylene glycol)s, or amines.[19]

Polymer colloids cover a broad field of self-assembling or self-organizing polymeric systems in solutions that possess surface-active or colloidal properties. Polymer colloids can be obtained by soapfree emulsion polymerization in aqueous media.[20,21] The colloids have a spherical shape with dimensions in the range of several hundred nanometers. Their stability is given by the dielectric layer induced by the charge of the initiator. Because of the relatively small dimensions of the colloids, their surface area is high and can act as support for the deposition of nanoparticles as a result of adhesion forces, allowing the formation of core−shell structures.[22,23] Thus, the shell comprised of nanoparticles is stabilized by the attraction forces present at the colloid surface, affording a hybrid material stable in aqueous media. An important advantage of the polymer colloids dispersed in aqueous media is the lack of toxicity, which allowed their use in different domains.[24,25]

Received: January 8, 2014
Accepted: September 18, 2014
Published: September 18, 2014

 © 2014 American Chemical Society

Table 1. Antimicrobial Activity Results; Silver Content and Overall Silver Release

		Staphylococcus aureus		*Escherichia coli*				.	
no.	sample	average diameter of the inhibition zone (mm)	standard deviation	average diameter of the inhibition zone (mm)[a]	standard deviation[a]	silver content for sample[b] (μg/g)	overall silver migration[c] (%)	standard deviation[a] for silver content	standard deviation for overall silver migration
1	A, in situ generated AgNPs	8.80	0.41	7.86	0.35	229.4	12.21	0.03	0.07
2	B, ex situ generated AgNPs	11.53	0.51	9.73	0.45	219	18.05	0.05	0.06
3	C, hybrid material without AgNPs	7.86	0.35	7.20	0.41			0.02	0.01

[a]Antimicrobial activity (average diameter and standard deviation) was determined using five membranes for each type and three discs (analysis) for each membrane. [b]Determined by ICP-MS. [c]Determined according to standard EN 1186-1:2002.

The aim of this study is to obtain a membrane with antimicrobial properties. A membrane material is a selective barrier for a certain species of molecules, ions, and particles, which is found at the interface of two different phases. Among the known functional materials, membranes show the greatest advantage, by associating their properties and characteristics that they have, the term "selectivity". The membrane significance is given also by the fact that they are considered as being the first functional materials ever existing on our planet—the membrane of the first unicellular organism.[26] The use of silver nanoparticles (AgNPs) as active agents in membranes is faced with the problem of nanoparticles immobilization, to reduce their leaching out[27] or aggregation during the filtration process.

There are several methods for the incorporation of nanoparticles in the membrane structure.[28] The main routes consist of the incorporation of nanoparticles generated in situ or ex situ during the membrane synthesis.[27] In the first approach, the synthesis of AgNPs is based on the reduction of ionic silver by the polymer solvent followed by the casting of the membrane.[27,29] The size and shape of the nanoparticles will depend on the relative rates of nucleation, growth, and stabilization. The ex situ method can also involve surface functionalization of the antimicrobial nanoparticles, which can aid during the membrane polymerization process.[30] Nevertheless, the main drawback consists of the leakage of the AgNPs from the membrane, caused by the direct contact with the contaminated fluids, remains to be solved.

Taking into consideration that the polymer colloids can act as a support, the adhesion of AgNPs onto the surface of polymer colloids can prove to be a viable alternative for enhancing the lifetime of the active layer. Nevertheless, the polymer colloids−AgNPs assembly needs to be stabilized to achieve a sustainable filtration process. For this purpose, multiwall carbon nanotobes (MWCNTs) were employed for the design of a networked structure with the polymer spheres covered with AgNPs.

Nanocomposites based on MWCNTs have gained intense interest owing to their improved properties, namely, mechanical behavior, thermal and electrical conductivities, and also high chemical stability.[31,32] Although MWCNTs have been correlated with ecotoxical effects,[33] DNA damage,[34] and pulmonary inflammation,[35] recent studies revealed that MWCNTs can be used in materials designed for water disinfection and purification[36] and coupled with AgNPs for photodegradation processes[37] or as fillers with antimicrobial activity.[38]

Scheme 1. Antimicrobial Membrane Design

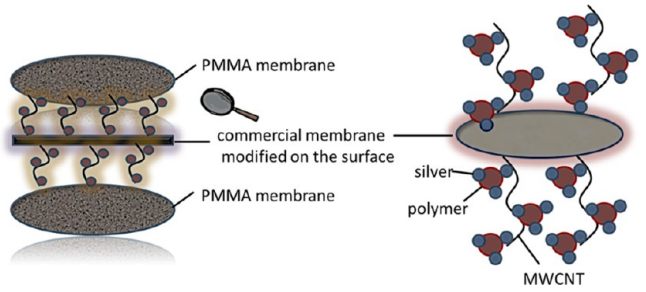

An optimum antimicrobial membrane design with possible uses in water purification should involve low-cost materials and increased lifetime service. Thus, the aim of our design is to try to satisfy these actual social and economic requirements.

To achieve these goals, we created a design that involves the use of different solutions and materials to attain different advantages: (1) The adhesion of the AgNPs to the polymer colloids bearing functional groups, to limit their leakage during the filtration process and to obtain a high surface area[23]; (2) creating a networked system between the polymer colloids with the aid of MWCNTs, thus obtaining an increased mechanical resistance as well as the integration of MWCNTs into the system[39]; (3) the use of a commercial membrane support for the deposition of an active antimicrobial layer, resulting also in an increase of the hydrophilicity; (4) encapsulation of the new system in a poly(methyl methacrylate) (PMMA) membrane for an increased lifetime.

The novelty of this study consists of the straightforward facile approach of creating the stable active antimicrobial membrane. The materials involved are easily obtainable and the manufacturing process is simple.

2. MATERIALS AND METHODS

2.1. Materials. Styrene (ST) (Merck) and acrylic acid (AA) (Sigma-Aldrich) have been purified through vacuum distillation. Potassium persulfate (KPS) (Merck) has been recrystallized from an ethanol/water mixture and then vacuum-dried. Hexane was dried by distillation on sodium and kept on 0.4 nm molecular sieves. 3-Bromopropan-1-ol (Aldrich), sodium azide (Fluka), diethyl ether (Fluka), acetone (Fluka), ethanol (Fluka), hydroxybenzotriazole (HOBt) (Aldrich), *N*-(3-(dimethylamino)-propyl) *N*′-carbodiimide (EDC) (Aldrich), 4-dimethylaminopyridine (Aldrich), silver nitrate ($AgNO_3$) (Aldrich), magnesium

Scheme 2. Antimicrobial Active Layer Preparation

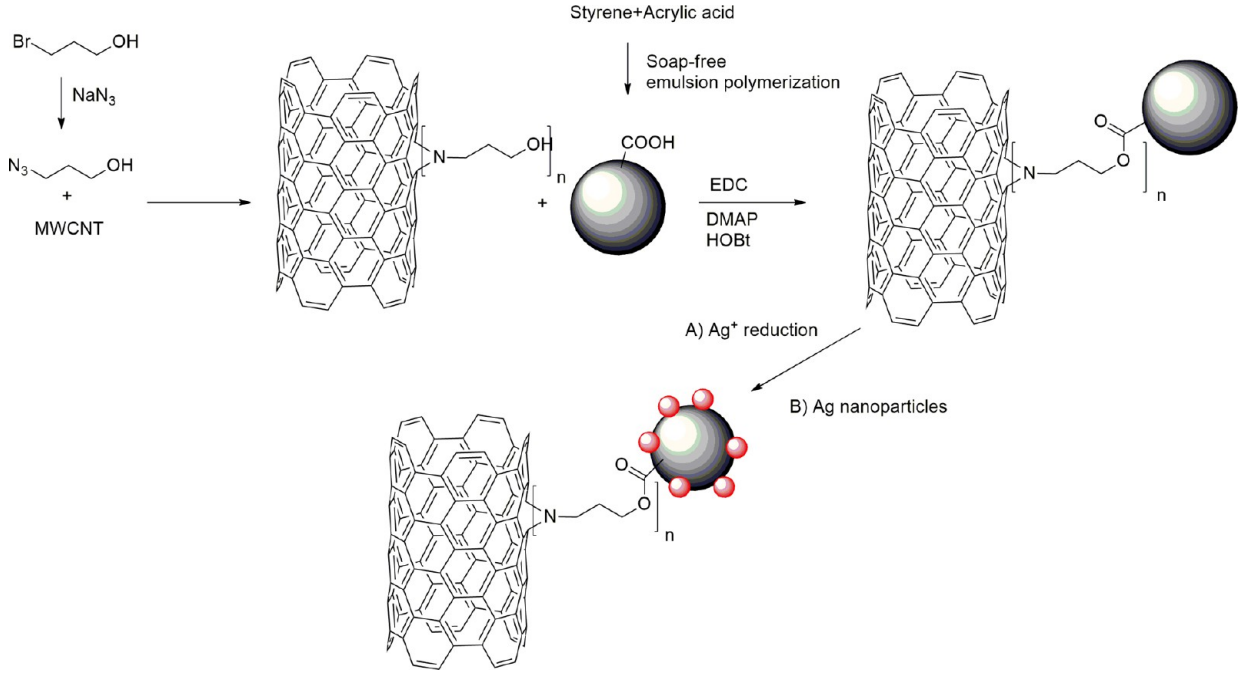

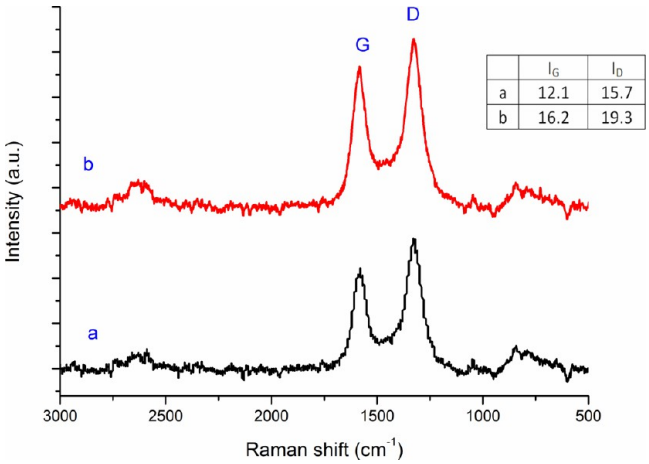

	I_G	I_D
a	12.1	15.7
b	16.2	19.3

Figure 1. Raman spectra for MWCNTs: (a) pristine MWCNTs and (b) modified MWCNTs (MWCNT−OH).

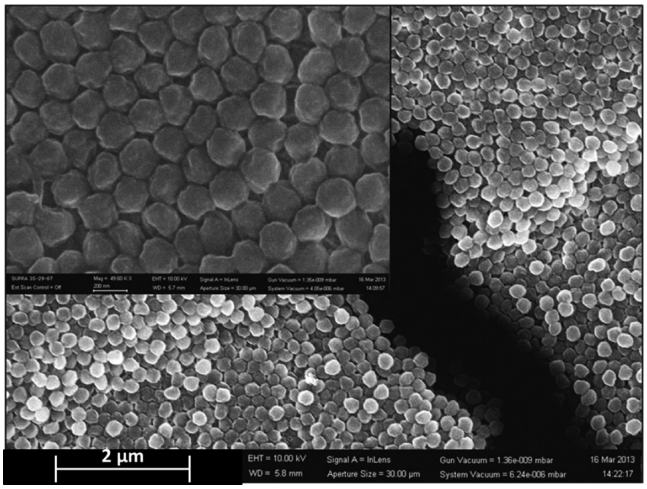

Figure 2. SEM images of ST−AA polymer particles.

sulfate (Merck), ascorbic acid (Merck), trisodium citrate dehydrate (Merck), sodium borohydride ($NaBH_4$) (Merck), chloroform (Fluka), and poly(methyl methacrylate) (PMMA) (M_w = 123000, Aldrich) were used without purification. MWCNTs (Sigma-Aldrich) with purity higher than 95% have been used as such. A commercial membrane of cellulose nitrate (Sartorius, Cellulose Nitrate Membrane Filter 11403Z-50-SCM) was used as supporting layer.

2.2. Methods. *2.2.1. Preparation of ST−AA Colloidal Particles Realized According to Previously Published Work.*[39] A 1.3 mL of ST and 0.2 mL of AA have been added to 20 mL of distilled water together with 0.0125 g of KPS. The reaction mixture has been nitrogen-purged and then maintained for 8 h at 75 °C under continuous stirring. The final dispersion has been dialyzed in distilled water for 7 days, using cellulose dialysis membranes (molecular weight cutoff: 12.000−14.000), to remove the unreacted monomer. The ST−AA polymer particles were recovered by latex deposition on a glass substrate (4 h at 60 °C).

2.2.2. 3-Azidopropan-1-ol Synthesized Starting from 3-Bromopropan-1-ol According to Literature.[40] 3-Bromo-propan-1-ol (5 g, 3.1 mL, 36 mmol) and sodium azide (3.9 g, 60 mmol) were dissolved in a mixture of acetone (60 mL) and water (10 mL) and the resulting solution was heated to reflux overnight. After partial removal of acetone under reduced pressure, 30 mL of water was added and the mixture was extracted with diethyl ether (4 × 40 mL). The organic layers collected were dried over $MgSO_4$ and the solvent was removed under reduced pressure to give a product as colorless oil (3.48 g, yield: 95%). ^{1}H NMR ($CDCl_3$, 300 MHz): δ = 3.75 (t, J = 6.0 Hz, CH_2−OH), 3.45 (t, J = 6.0 Hz, CH_2−N_3), 1.83 (q, J = 6.0 Hz, 2H, $CH_2CH_2CH_2$), 1.70 (s, CH_2−OH).

2.2.3. Synthesis of Hydroxyl-Functionalized MWCNTs (MWCNTs−OH). Pristine MWCNTs (0.066 g) and 3-azido-propan-1-ol (0.6 g) were added in 11 mL of dichlorobenzene, under a nitrogen atmosphere. The mixture was stirred at 80 °C overnight, after which it was precipitated in 40 mL of diethyl

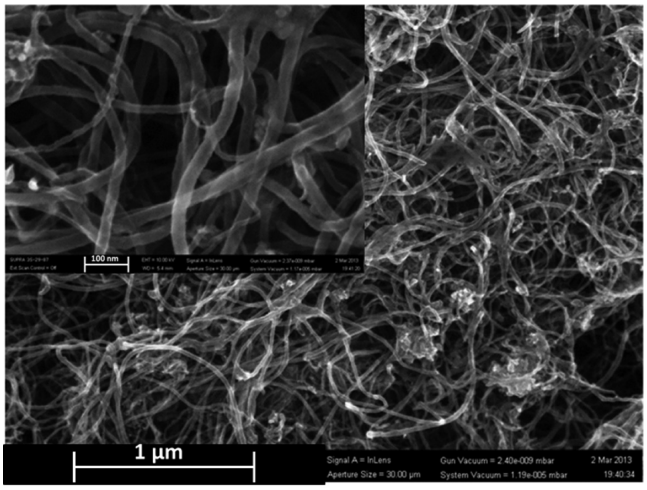

(a)

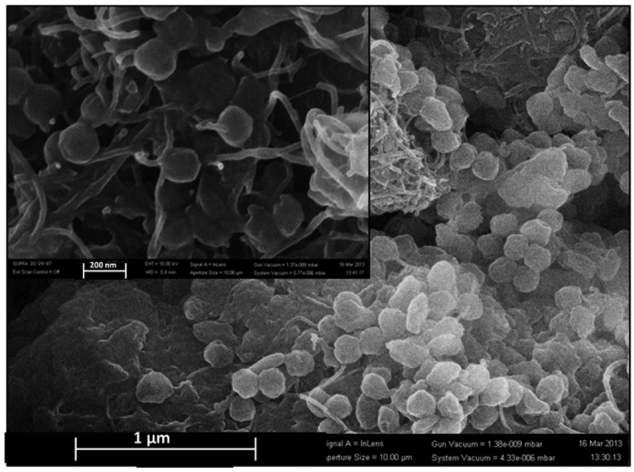

(b)

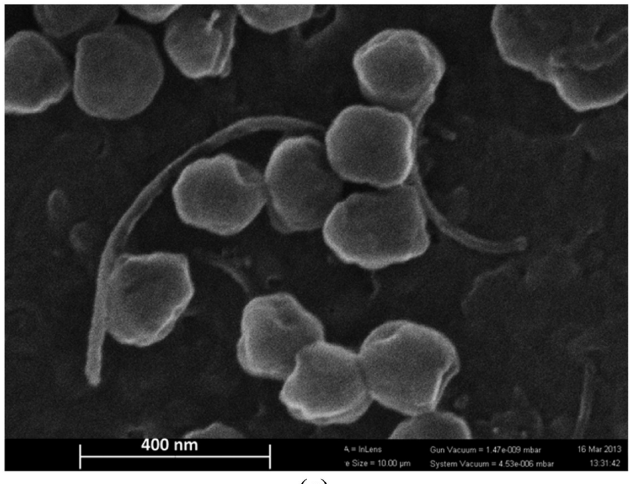

(c)

Figure 3. SEM images (a) MWCNTs−OH; (b) and (c) hybrid material.

ether. The hydroxyl-functionalized MWCNTs (MWCNTs−OH) were recovered by filtration and washing with diethyl ether.

2.2.4. Synthesis of Hybrid Material ST−AA−MWCNTs. To a degassed solution of polymer particles ST−AA (450 mg) in dry hexane (12.5 mL) was added HOBt (23 mg, 0.17 mmol), EDC (256 120 μL, 0.669 mmol), 4-dimethylaminopyridine (DMAP)

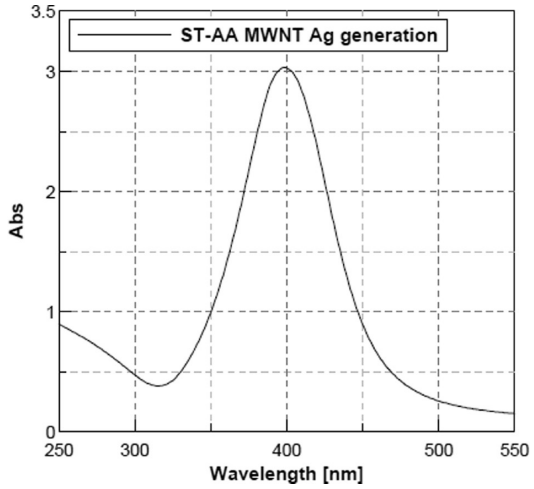

Figure 4. UV−vis analysis of in situ generated AgNPs.

(27 mg, 0.223 mmol), and 15 mg of MWCNTs−OH dispersed in 2.5 mL of dry hexane. The mixture was stirred at room temperature under nitrogen for 2 days. The mixture was filtrated and purified by repeated washing with ethanol, followed by drying at 70 °C (4 h).

2.2.5. AgNPs In Situ Generation. ST−AA−MWCNTs hybrid material (21.9 mg) was dispersed in 10 mL of H_2O. To this dispersion ascorbic acid (5 mg, 0.028 mmol) and trisodium citrate (5 mg, 0.017 mmol) were added, after which a solution of $AgNO_3$ (8 mg, 0.045 mmol) in 0.5 mL of H_2O was introduced in the reaction. The mixture was stirred at room temperature for 30 min. The obtained solution was used for the realization of the membrane active layer (layer A) by dip-coating method and dried at room temperature.

2.2.6. AgNPs Ex Situ Generation. Trisodium citrate (2.5 mmol, 0.735 g) was added to a solution of $AgNO_3$ (2.5 mmol, 0.425 g) in 100 mL of water and stirring was continued for 30 s. Subsequently, a solution of $NaBH_4$ (0.3 mmol, 0.012 g) in 3 mL of water was introduced and the mixture was stirred for 60 s at room temperature. The solution developed a yellow coloration as a result of formation of AgNPs and was stored in a brown bottle at 4 °C.

2.2.7. Membrane Active Layer Preparation, Using Ex Situ Generated AgNPs (Layer B). The preparation of the active layer involved the use of solutions containing 30 mg of ST−AA−MWCNTs dispersed by ultrasonication in 4 mL of AgNPs solution generated ex situ. The obtained dispersions were deposited on the commercial membrane by dip-coating method and dried at room temperature.

2.2.8. PMMA Encapsulating Membrane. The realization of the encapsulating membrane involved the use of a 5% PMMA solution in a chloroform/ethanol (2:1 v/v) mixture and evaporation at room temperature.

2.3. Characterization. The Raman spectra have been registered on a DXR Raman Microscope from Thermo Scientific with a 633 nm laser. The laser beam has been focused with a 10× objective.

XPS (X-ray photoelectron microscopy) analysis was performed on a K-Alpha instrument from Thermo Scientific, using a monochromated Al Kα source (1486.6 eV), at a low pressure of 2×10^{-9} mbar. Charging effects were compensated for by a flood gun, and binding energy was calibrated by placing the C 1s peak at 285 eV as internal standard. The survey spectra were obtained using a pass energy of 200 eV and for the

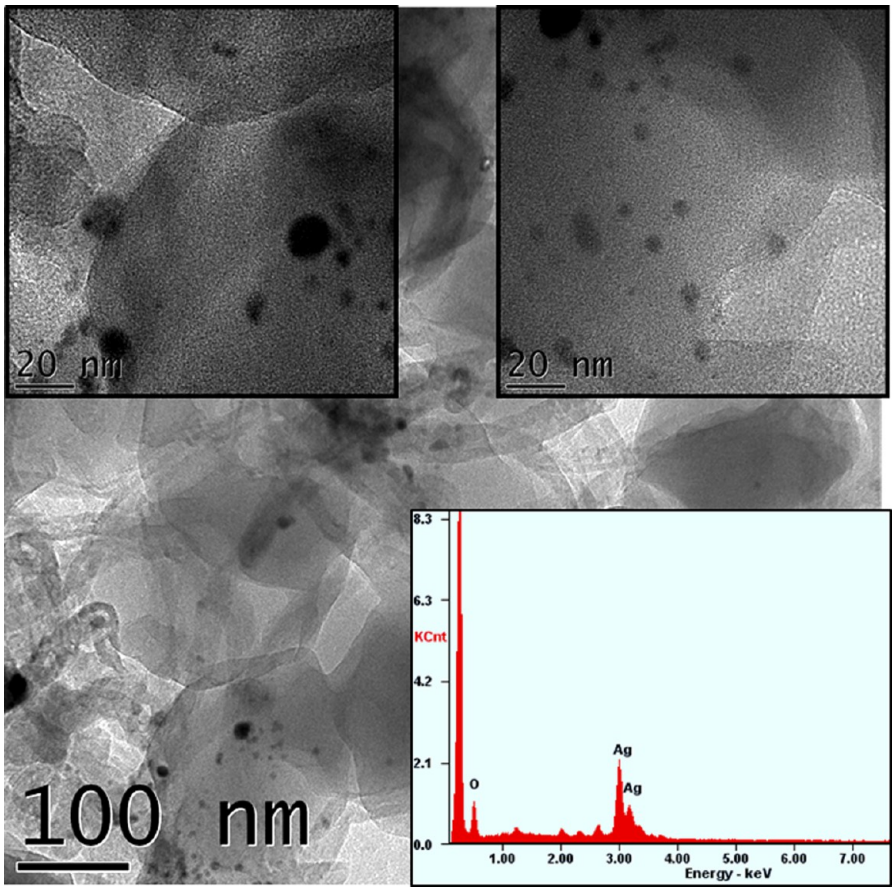

Figure 5. TEM images of the hybrid material presenting in situ generated AgNPs (A).

high-resolution spectra a 50 eV pass energy and 100 scans. The deconvolution of the N 1s peak was performed after subtraction of a Smart background.

The TGA analysis has been performed on Q500 TA Instruments equipment, under oxygen atmosphere, using a heating rate of 20 °C/min from room temperature to 900 °C.

The infrared absorption spectra have been recorded at room temperature with a Nicolet 6700 FTIR spectrometer in the range of 4000−400 cm^{-1}.

For the morphological characterization of the obtained materials scanning electron microscopy analyses were performed using a FE-SEM (field emission-scanning electron microscope) - RAITH e_Line at 10 kV acceleration voltage.

The UV−vis absorption spectra were recorded using a V-500 Able Jasco spectrophotometer.

The high-resolution transmission electron microscopy (HRTEM) studies were performed on an atomic resolution analytical JEOL JEM-ARM 200F electron microscope, operating at 200 kV. Specimens for TEM were prepared in the following way: 0.02 mL of concentrated liquid sample ST−AA−MWCNTs−Ag mixture was diluted with 5 mL of bidistilled water and further dispersed by sonication for 5 min; a drop from the dispersed hybrid material was put on carbon-coated copper grids and let dry in air on filter paper.

The particles size distribution were measured through dynamic light scattering (DLS) with a Nani ZS device (redbadge).

2.3.1. Antimicrobial Activity Determination. Antimicrobial activity determination was tested using *Staphylococcus aureus,* ATCC 25923, using a testing protocol similar to Kirby-Bauer[41] disc diffusion test in an agar medium. Bacterium taken from an overnight MHB culture was freshly grown for 4 h having approximately 10^6 CFU/mL. With this culture, a bacterial lawn was prepared on plate counter agar. Membrane discs (the modified commercial membrane) of 6 mm size were used to observe susceptibility patterns against the different loading of the active layer (A, in situ generated AgNPs; B, ex situ generated AgNPs; C, hybrid material without AgNPs). A set containing two membrane discs for each active layer was tested.

2.3.2. Determination of Silver Content. Determination of silver content was realized using an inductively coupled plasma-mass spectrometer (ICP-MS) NexIon 300q (Perkin-Elmer) using a procedure similar to that of Lin et al.[42] The calibration curve was realized using a multielement standard 5% HNO_3 matrix from Perkin-Elmer with a silver concentration of 10 mg/L.

a. Sample Preparation for Mineralization—Determination of Total Silver Concentration. Membrane discs of systems A, B, and C were precisely weighted (7.7, 8.2, and 7.5 mg, respectively) and introduced in Teflon flasks and 4 mL of HNO_3 and 2 mL of H_2O_2. The digestion was realized in a microwave reactor MWS-2 (Berghof, 1000 W). The digestion program was as follows: stage 1, 5 min at 160 °C (80% power); stage 2, 40 min at 220 °C (80% power); stage 3, 20 min for cooling. After mineralization, the samples were diluted to 10 mL with ultrapure water. The obtained solution was analyzed by ICP-MS. To verify the accuracy of this method, three samples containing different quantities of $AgNO_3$, a commercial AgNP solution, have been analyzed. The error was around 0.67−0.70%.

b. Sample Preparation—Determination of Silver Migration. The migration of silver from the samples was determined

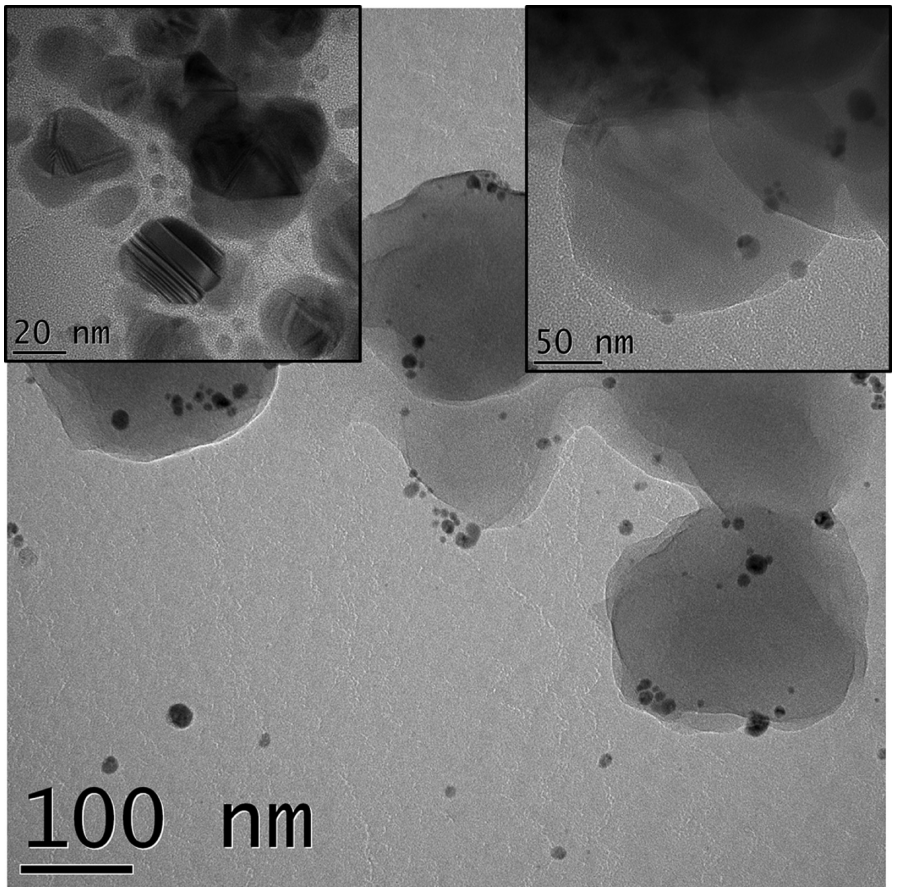

Figure 6. TEM images of the hybrid material obtained using ex situ synthesized AgNPs (B).

by extraction with ultrapure water according to standard EN 1186-1:2002 (materials and articles in contact with foodstuffs—"Plastics-Part 1: Guide to the selection of conditions and test methods for overall migration"). Samples of 3.25 cm^2 were extracted using 32.5 cm^3 distilled water (1:10, sample surface: volume ratio). The extraction conditions were: 2 h at 80 °C. After extraction the samples were removed and the solution was acidified with 1% HNO_3 and analyzed by ICP-MS. The results are presented in Table 1.

3. RESULTS AND DISCUSSION

Membranes with antimicrobial activity presenting a complex sandwich-type structure (Scheme 1) have been obtained. The outer layers are comprised of PMMA membranes, whereas the inner active layer consists of a modified commercial membrane to achieve antimicrobial properties. This characteristic is a result of the presence of AgNPs in the active antimicrobial layer deposited on the commercial membrane. This hybrid material consists of polymer colloids and MWCNTs which have been used for the stabilization of the active layer, respectively, for the interconnection/joining of the polymer particles (Scheme 1).

The methodology used for the synthesis of the active layer is presented in Scheme 2. The first step has been the obtaining of an azido alcohol and its reaction with the MWCNTs, resulting in a highly dispersible product both in aqueous and organic solvents. This facilitated the next stage consisting of the esterification reaction with the carboxyl groups present at the surface of the polymer particles. This hybrid material has served as support for the fixation of nanoparticles with antimicrobial activity by employing two synthesis strategies: (A) the in situ generation of AgNPs in the presence of the hybrid material and (B) realization of a physical mixture with preformed AgNPs (Scheme 2).

The hydroxyl-functionalized MWCNTs (MWCNT−OH) were synthesized using the reactivity of the azide groups which realize a covalent bond with MWCNTs.[43,44] Thus, by employing an azido alcohol, the surface of the MWCNT will present free hydroxyl groups.[45]

Therefore, the first stage of this study consisted of the obtaining of the azido $HO-C_3-N_3$ derivative and its characterization by ^1H NMR. The recorded signals were in $CDCl_3$ at 300 MHz: δ 3.77 (q, 2H, J = 5.8 Hz, CH_2-OH), 3.47 (t, 2H, J = 6.5 Hz, CH_2-N_3), 1.85 (quint, 2H, J = 6.0 Hz, $CH_2CH_2CH_2$), confirming the desired structure[40] (for spectra see Supporting Information).

To determine the covalent modification of the MWCNTs with the azido alcohol, Raman and XPS analyses were performed (see Figure 1 and Supporting Information). First-order Raman spectroscopy showed a strong band at 1580 cm^{-1} (G band), which was the Raman allowed phonon high-frequency mode and a disordered-induced peak at 1330 cm^{-1} (D band), which originates from defects in the curved graphene sheets and at tube ends. Comparing the I_D/I_G ratios of the samples, which were 1.30 for MWCNTs before functionalization and 1.19 for that after treatment, revealed that the chemical modification increased the degree of the disorder, but no damages occurred to MWCNTs through functionalization.[46] From the XPS analysis we have calculated a modification degree of 4.2% (please see Figure S2 of the Supporting Information).

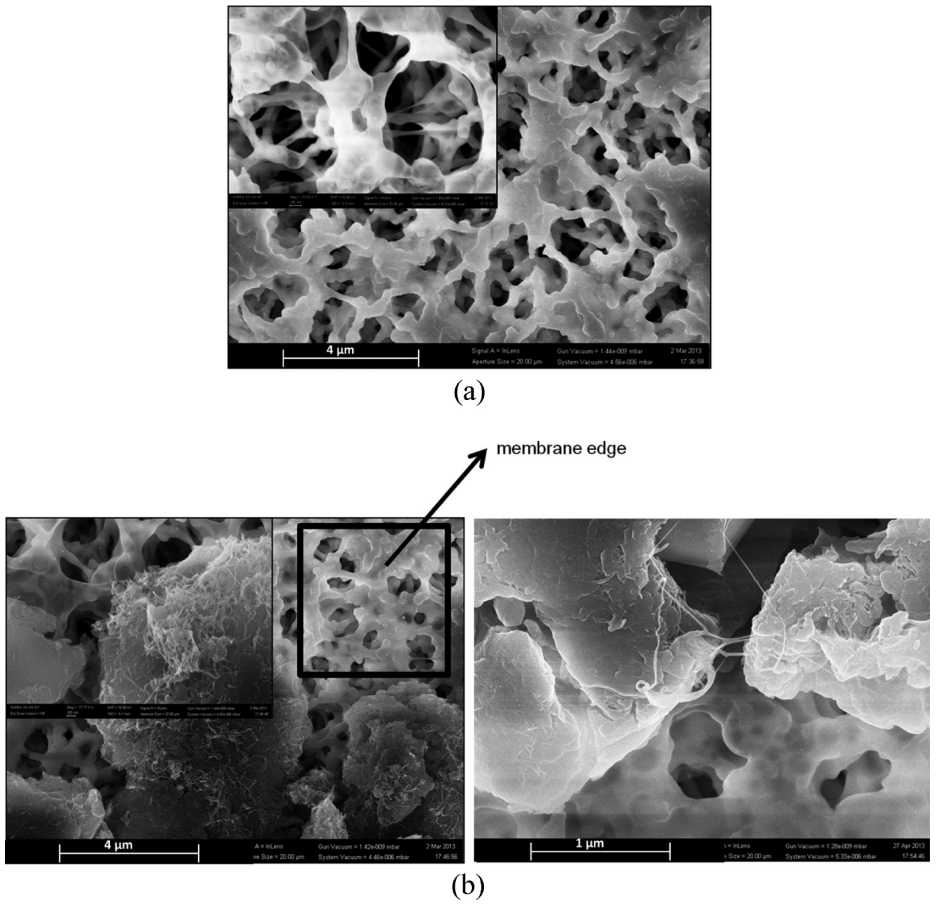

Figure 7. Active layer deposition: (a) initial structure of the membrane; (b) active layer deposits on the commercial membrane surface.

Soapfree emulsion polymerization of the styrene−acrylic acid system affords polymer colloids presenting carboxyl groups at their surface.[47−49] The scanning electron microscopy (SEM) analysis of the particles revealed that the average diameter is around 200 nm (Figure 2).

The next step consisted of the linking of the polymer particles to the MWCNTs−OH by an esterification reaction of the carboxyl groups present on the colloids with the hydroxyl groups present on the modified MWCNTs. FT-IR spectroscopy was employed for the characterization of the obtained material, which revealed the appearance of a signal at 1235 cm^{-1} specific to the vibration of C−O from the ester group. SEM analysis was performed for the morphology characterization of the material (Figure 3).

The analysis of Figure 3 reveals that the MWCNTs−OH are no longer bundled together but more distanced one from the other and the polymer particles are attached to their surface. Also, hybrid agglomerates are formed, consisting of MWCNTs and polymer particles which represent a confirmation of the stabilization of the system realized through the esterification reaction. This networked structure is necessary due to the fact that the polymer colloids are smaller than the pores of the commercial membrane. Thus, without the connection between the MWCNTs−OH and the colloids, the polymer particles would detach and would be lost during the filtration process.

To attain high antimicrobial activity, AgNPs were added to the obtained system. The first approach consisted of the in situ generation of AgNPs. The UV−vis analysis (Figure 4) of the resulting system revealed the presence of an absorption band at 400 nm, confirming the generation of AgNPs.

Transmission electron microscopy (TEM) analysis was performed for the morphological characterization of the hybrid material containing the in situ synthesized AgNPs (A).

The analysis of Figure 5 reveals that both the polymer particles and the MWCNTs are covered with AgNPs, which are present either as aggregates or as individual particles with an average diameter of 5 nm. The EDX analyses confirm the obtaining of AgNPs.

The second method for AgNPs addition to the hybrid material was the realization of a physical mixture of ex situ synthesized AgNPs and the polymer colloids/MWCNTs aqueous dispersion (B). For the morphological characterization, TEM analysis was performed.

The TEM analysis of system B (Figure 6) reveals a higher dimensional polydispersity of the AgNPs which have diameter value between 20 and 40 nm. The major difference between systems A and B is the localization of AgNPs predominantly on the hybrid material for (A) whereas for (B) isolated silver AgNPs are formed in regions between the polymer colloids/MWCNTs hybrid material. This aspect can be explained by the stronger adhesion forces present in system A as a result of the smaller particle size for the AgNPs produced by the in situ synthesis process. Thus, in the case of system A, the AgNPs formation rate allows the fixation of silver clusters onto the polymer colloids surface, leading to an AgNPs growth process predominantly on the polymer particles. In the case of system B the formation of insular agglomerates can be explained by their synthesis in the presence of a stabilizing agent which does not allow the total adhesion on the surface of the hybrid material.

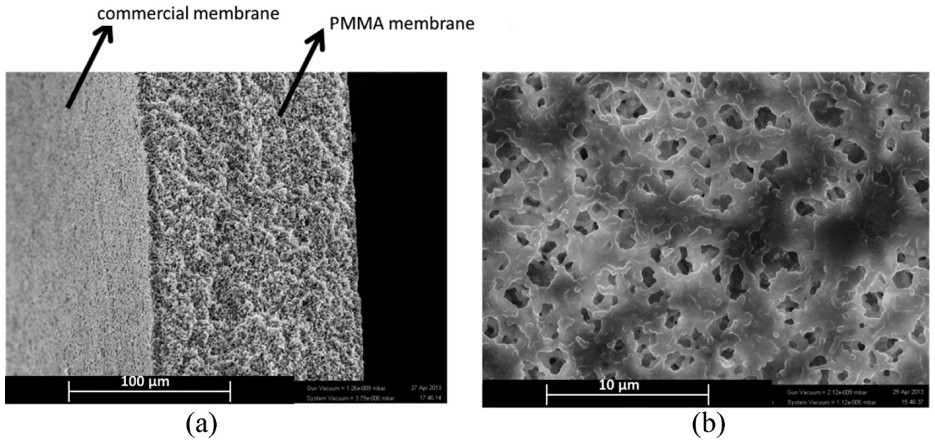

Figure 8. SEM images of the final encapsulated membrane: (a) cross-section image; (b) image of the PMMA porous layer.

The next stage of the study consists of the surface modification of a commercial hydrophilic membrane using the aqueous dispersion of system A or B. The fabrication process involved the producing of an active layer on both faces of the commercial membrane.

The morphology of the modified membrane surface was investigated by SEM (Figure 7). The initial membrane is presented in Figure 7a, which reveals the highly ordered porous structure, with an average pore size of 1 μm. From the investigation of images in Figure 7b, one can conclude that the active layer covers almost the entire membrane surface with some deficits/shortages at the edges of the membrane disc, as it resulted from the dip-coating deposition method. Nevertheless, the incomplete covered area represents only a very small percentage.

The active layer adhesion to the commercial membrane is not sufficient to ensure a long-life material. To resolve this problem, the modified membrane was "encapsulated" using a PMMA membrane. The images of this encapsulating membrane and of the cross section of the final membrane structure are presented in Figure 8.

The pores of the obtained PMMA membrane have a diameter around 1 μm, as can be observed from Figure 8b. The overall porosity of the obtained sandwich-type structure can be assessed from Figure 8a, which reveals a more compact porous structure in the case of the modified commercial membrane. This represents an important advantage for the filtration process, allowing a longer contact time between the filtrate and the antimicrobial active layer.

In Figure 9 are presented the results obtained during continuous filtration tests using commercial membrane as reference. The fluxes were measured using a Sartorius module (the membrane is fixed on the support and the cross-flow is vertical to the entire membrane surface) at 0.1 atm pressure. The used solvents (500 mL) for determinations were deionized water and absolute ethanol. Usually, the ethanol fluxes are higher than the water fluxes, which is also valid here in the case of the cellulose nitrate membrane. For the composite membranes the water flux is higher than the ethanol flux for both types of AgNPs-containing membranes. This can be explained by the higher hydrophilicity of the active layer (the colloid particles, silver nanoparticles, and the MWCNTs−OH) from the composite membrane structure. Another observation that can be made is that the variation of fluxes in time is low, even for the synthesized material, this being proof of the composite membrane cross-section stability.

For the determination of the antimicrobial activity, the obtained complex membranes have been tested using *Staphylococcus aureus*, ATCC 25923, and *Escherichia coli*, ATCC 25922, using a disc diffusion procedure. The growth inhibition diameters (including the diameter of the 6 mm discs), measured

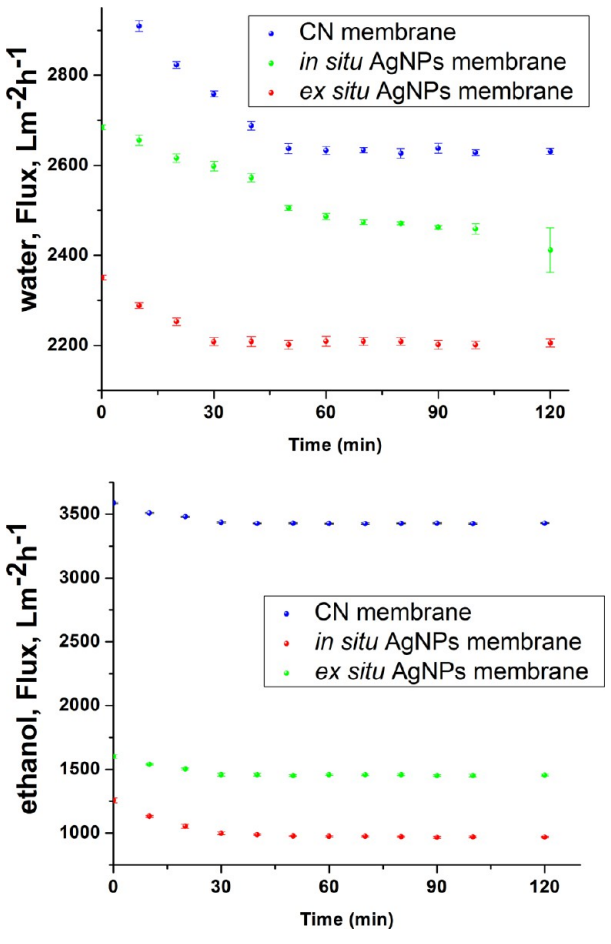

Figure 9. Continuous filtration tests using deionized water and absolute ethanol for the testing of the composite membrane and the commercial (cellulose nitrate) membrane. The error bar was determined after the fabrication of five membranes for each AgNPs type, thus indicating the good reproducibility of the results.

dx.doi.org/10.1021/am505024p | *ACS Appl. Mater. Interfaces* 2014, 6, 17384−17393

after 2 days, are presented in Table 1. Silver content and release rate are the determining factors for the antimicrobial activity. For this reason, we have employed ICP-MS to determine the silver concentration in each system and to evaluate the migration rate (Table 1).

The results show good antimicrobial activity toward *S. aureus* and *E. coli* for the samples containing ex situ generated AgNPs, which can be explained by the higher relative silver release rate. Although system A presents a slightly higher silver concentration, the antimicrobial activity decrease is explained by the lower relative silver migration. This can be explained by a higher adhesion of the in situ generated AgNPs to the polymer colloids which limits their diffusion.

4. CONCLUSIONS

We have realized a membrane with antimicrobial activity using a new strategy consisting of the realization of a sandwiched-type structure based on polymer colloids, MWCNTs, and AgNPs.

The employed manufacturing process involved the transformation/augmentation of commercial membrane supports, to attain antimicrobial activity. The AgNPs have been immobilized using polymer colloids presenting carboxyl groups which gave rise to good adhesion properties for the nanoparticles. The polymer colloids/AgNPs have been stabilized by the realization of a networked structure involving MWCNTs.

The filtration tests revealed good stability of the materials and increased hydrophilicity of the hybrid membranes. The antimicrobial properties have been evaluated using *Staphylococcus aureus* and have been correlated with the migration rate of silver ions.

The membrane new design permits the obtaining of good antimicrobial properties and good filtration stability by employing facile manufacturing processes.

■ ASSOCIATED CONTENT

Ⓢ Supporting Information

^{1}H NMR for the 3-azido-propan-1-ol, XPS deconvolution for N 1s, for the MWCNT−OH, TGA analysis of MWCNT and MWCNT−OH, and DLS analysis−histogram for ex situ synthesized AgNPs. This material is available free of charge via the Internet at http://pubs.acs.org/.

■ AUTHOR INFORMATION

Corresponding Author

*E-mail: aurel_diacon@yahoo.com. Tel.: +40 021 402 2708.

Notes

The authors declare no competing financial interest.

■ ACKNOWLEDGMENTS

A.D. and A.M. acknowledge financial support from the Sectoral Operational Programme Human Resources Development 2007−2013 of the Ministry of European Funds through the Financial Agreement POSDRU/159/1.5/S/132395 and POSDRU/159/1.5/S/132397. L.C.N. acknowledges the Core Program no. PN09-450103 of the National Authority for Scientific Research from the Ministry of Education and Youth of Romania.

■ REFERENCES

(1) Kim, J. S.; Kuk, E.; Yu, K. N.; Kim, J.-H.; Park, S. J.; Lee, H. J.; Kim, S. H.; Park, Y. K.; Park, Y. H.; Hwang, C.-Y.; Kim, Y.-K.; Lee, Y.-S.; Jeong, D. H.; Cho, M.-H. Antimicrobial Effects of Silver Nanoparticles. *Nanomedicine (N. Y., NY, U. S.)* **2007**, *3*, 95−101.

(2) Jones, S. A.; Bowler, P. G.; Walker, M.; Parsons, D. Controlling Wound Bioburden with a Novel Silver-Containing Hydrofiber® Dressing. *Wound Repair Regen.* **2004**, *12*, 288−294.

(3) Ilić, V.; Šaponjić, Z.; Vodnik, V.; Potkonjak, B.; Jovančić, P.; Nedeljković, J.; Radetić, M. The Influence of Silver Content on Antimicrobial Activity and Color of Cotton Fabrics Functionalized with Ag Nanoparticles. *Carbohydr. Polym.* **2009**, *78*, 564−569.

(4) Kelly, P. J.; Li, H.; Benson, P. S.; Whitehead, K. A.; Verran, J.; Arnell, R. D.; Iordanova, I. Comparison of the Tribological and Antimicrobial Properties of CrN/Ag, ZrN/Ag, TiN/Ag, and TiN/Cu Nanocomposite Coatings. *Surf. Coat. Technol.* **2010**, *205*, 1606−1610.

(5) Lin, S.; Huang, R.; Cheng, Y.; Liu, J.; Lau, B. L. T.; Wiesner, M. R. Silver Nanoparticle-Alginate Composite Beads for Point-of-Use Drinking Water Disinfection. *Water Res.* **2013**, *47*, 3959−3965.

(6) Perera, S.; Bhushan, B.; Bandara, R.; Rajapakse, G.; Rajapakse, S.; Bandara, C. Morphological, Antimicrobial, Durability, and Physical Properties of Untreated and Treated Textiles Using Silver-Nanoparticles. *Colloids Surf., A* **2013**, *436*, 975−989.

(7) Tran, Q. H.; Nguyen, V. Q.; Le, A.-T. Silver Nanoparticles: Synthesis, Properties, Toxicology, Applications and Perspectives. *Adv. Nat. Sci.: Nanosci. Nanotechnol.* **2013**, *4*, 033001.

(8) Zhang, Y.; Peng, H.; Huang, W.; Zhou, Y.; Yan, D. Facile Preparation and Characterization of Highly Antimicrobial Colloid Ag or Au Nanoparticles. *J. Colloid Interface Sci.* **2008**, *325*, 371−376.

(9) Panáček, A.; Kvítek, L.; Prucek, R.; Kolář, M.; Večeřová, R.; Pizúrová, N.; Sharma, V. K.; Nevěčná, T. j.; Zbořil, R. Silver Colloid Nanoparticles: Synthesis, Characterization, and Their Antibacterial Activity. *J. Phys. Chem. B* **2006**, *110*, 16248−16253.

(10) Peetsch, A.; Greulich, C.; Braun, D.; Stroetges, C.; Rehage, H.; Siebers, B.; Köller, M.; Epple, M. Silver-Doped Calcium Phosphate Nanoparticles: Synthesis, Characterization, and Toxic Effects Toward Mammalian and Prokaryotic Cells. *Colloids Surf., B* **2013**, *102*, 724−729.

(11) Zhang, W.; Qiao, X.; Chen, J. Synthesis and Characterization of Silver Nanoparticles in AOT Microemulsion System. *Chem. Phys.* **2006**, *330*, 495−500.

(12) Darroudi, M.; Khorsand Zak, A.; Muhamad, M. R.; Huang, N. M.; Hakimi, M. Green Synthesis of Colloidal Silver Nanoparticles by Sonochemical Method. *Mater. Lett.* **2012**, *66*, 117−120.

(13) Byeon, J. H.; Kim, Y.-W. A Novel Polyol Method to Synthesize Colloidal Silver Nanoparticles by Ultrasonic Irradiation. *Ultrason. Sonochem.* **2012**, *19*, 209−215.

(14) Lengke, M. F.; Fleet, M. E.; Southam, G. Biosynthesis of Silver Nanoparticles by Filamentous Cyanobacteria from a Silver(I) Nitrate Complex. *Langmuir* **2007**, *23*, 2694−2699.

(15) Choi, S.-H.; Zhang, Y.-P.; Gopalan, A.; Lee, K.-P.; Kang, H.-D. Preparation of Catalytically Efficient Precious Metallic Colloids by γ-Irradiation and Characterization. *Colloids Surf., A* **2005**, *256*, 165−170.

(16) Yang, K.-H.; Chang, C.-M. Using a Photochemical Method and Chitosan to Prepare Surface-Enhanced Raman Scattering−Active Silver Nanoparticles. *Anal. Chim. Acta* **2012**, *729*, 1−6.

(17) Battocchio, C.; Meneghini, C.; Fratoddi, I.; Venditti, I.; Russo, M. V.; Aquilanti, G.; Maurizio, C.; Bondino, F.; Matassa, R.; Rossi, M.; Mobilio, S.; Polzonetti, G. Silver Nanoparticles Stabilized with Thiols: A Close Look at the Local Chemistry and Chemical Structure. *J. Phys. Chem. C* **2012**, *116*, 19571−19578.

(18) Kashiwagi, Y.; Yamamoto, M.; Nakamoto, M. Facile Size-Regulated Synthesis of Silver Nanoparticles by Controlled Thermolysis of Silver Alkylcarboxylates in the Presence of Alkylamines with Different Chain Lengths. *J. Colloid Interface Sci.* **2006**, *300*, 169−175.

(19) Yamamoto, M.; Nakamoto, M. Novel Preparation of Monodispersed Silver Nanoparticles via Amine Adducts Derived from Insoluble Silver Myristate in Tertiary Alkylamine. *J. Mater. Chem.* **2003**, *13*, 2064−2065.

(20) Rusen, E.; Mocanu, A.; Corobea, C.; Marculescu, B. Obtaining of Monodisperse Particles Through Soap-Free Polymerization in the Presence of C60. *Colloids Surf., A* **2010**, *355*, 23−28.

(21) Herzog Cardoso, A.; Leite, C. A. P.; Zaniquelli, M. E. D.; Galembeck, F. Easy Polymer Latex Self-Assembly and Colloidal Crystal Formation: The Case of Poly[styrene-co-(2-hydroxyethyl Methacrylate)]. *Colloids Surf., A* **1998**, *144*, 207−217.
(22) Taniguchi, T.; Inada, T.; Kashiwakura, T.; Murakami, F.; Kohri, M.; Nakahira, T. Preparation of Polymer Core−Shell Particles Supporting Gold Nanoparticles. *Colloids Surf., A* **2011**, *377*, 63−69.
(23) Vasile, E.; Rusen, E.; Mocanu, A.; Patrascu, M.; Calinescu, I. Polymer Colloids and Silver Nanoparticles Hybrid Materials. *Colloid Polym. Sci.* **2012**, *290*, 193−201.
(24) Tapeinos, C.; Efthimiadou, E. K.; Boukos, N.; Charitidis, C. A.; Koklioti, M.; Kordas, G. Microspheres as Therapeutic Delivery Agents: Synthesis and Biological Evaluation of pH Responsiveness. *J. Mater. Chem. B* **2013**, *1*, 194−203.
(25) Mocanu, A.; Marculescu, B.; Somoghi, R.; Miculescu, F.; Boscornea, C.; Stancu, I. C. Fluorescence Enhancement for the Complex PAMAM−BSA in the Presence of Photonic Crystal Heterostructures. *Colloids Surf., A* **2011**, *392*, 288−293.
(26) Lehn, J.-M. Transport Processes and Carrier Design. In *Supramolecular Chemistry*; Wiley-VCH Verlag GmbH & Co. KGaA: Weinheim, 1995; Chapter 6, pp 69−80.
(27) Taurozzi, J. S.; Arul, H.; Bosak, V. Z.; Burban, A. F.; Voice, T. C.; Bruening, M. L.; Tarabara, V. V. Effect of Filler Incorporation Route on the Properties of Polysulfone−Silver Nanocomposite Membranes of Different Porosities. *J. Membr. Sci.* **2008**, *325*, 58−68.
(28) Ng, L. Y.; Mohammad, A. W.; Leo, C. P.; Hilal, N. Polymeric Membranes Incorporated with Metal/Metal Oxide Nanoparticles: A Comprehensive Review. *Desalination* **2013**, *308*, 15−33.
(29) Kim, J.; Van der Bruggen, B. The Use of Nanoparticles in Polymeric and Ceramic Membrane Structures: Review of Manufacturing Procedures and Performance Improvement for Water Treatment. *Environ. Pollut.* **2010**, *158*, 2335−2349.
(30) Zhang, G.; Lu, S.; Zhang, L.; Meng, Q.; Shen, C.; Zhang, J. Novel Polysulfone Hybrid Ultrafiltration Membrane Prepared with TiO2-g-HEMA and its Antifouling Characteristics. *J. Membr. Sci.* **2013**, *436*, 163−173.
(31) Spitalsky, Z.; Tasis, D.; Papagelis, K.; Galiotis, C. Carbon Nanotube−Polymer Composites: Chemistry, Processing, Mechanical and Electrical Properties. *Prog. Polym. Sci.* **2010**, *35*, 357−401.
(32) Tasis, D.; Tagmatarchis, N.; Bianco, A.; Prato, M. Chemistry of Carbon Nanotubes. *Chem. Rev.* **2006**, *106*, 1105−1136.
(33) Petersen, E. J.; Zhang, L.; Mattison, N. T.; O'Carroll, D. M.; Whelton, A. J.; Uddin, N.; Nguyen, T.; Huang, Q.; Henry, T. B.; Holbrook, R. D.; Chen, K. L. Potential Release Pathways, Environmental Fate, And Ecological Risks of Carbon Nanotubes. *Environ. Sci. Technol.* **2011**, *45*, 9837−9856.
(34) Ghosh, M.; Chakraborty, A.; Bandyopadhyay, M.; Mukherjee, A. Multi-Walled Carbon Nanotubes (MWCNT): Induction of DNA Damage in Plant and Mammalian Cells. *J. Hazard. Mater.* **2011**, *197*, 327−336.
(35) Porter, D. W.; Hubbs, A. F.; Mercer, R. R.; Wu, N.; Wolfarth, M. G.; Sriram, K.; Leonard, S.; Battelli, L.; Schwegler-Berry, D.; Friend, S.; Andrew, M.; Chen, B. T.; Tsuruoka, S.; Endo, M.; Castranova, V. Mouse Pulmonary Dose- and Time Course-Responses Induced by Exposure to Multi-Walled Carbon Nanotubes. *Toxicology* **2010**, *269*, 136−147.
(36) Liu, X.; Wang, M.; Zhang, S.; Pan, B. Application Potential of Carbon Nanotubes in Water Treatment: A Review. *J. Environ. Sci.* **2013**, *25*, 1263−1280.
(37) Yan, Y.; Sun, H.; Yao, P.; Kang, S.-Z.; Mu, J. Effect of Multi-Walled Carbon Nanotubes Loaded with Ag Nanoparticles on the Photocatalytic Degradation of Rhodamine B Under Visible Light Irradiation. *Appl. Surf. Sci.* **2011**, *257*, 3620−3626.
(38) Subbiah, R.; Veerapandian, M.; Sadhasivam, S.; Yun, K. Triad CNT-NPs/Polymer Nanocomposites: Fabrication, Characterization, and Preliminary Antimicrobial Study. *Synth. React. Inorg. Met. Org. Chem.* **2011**, *41*, 345−355.
(39) Mocanu, A.; Rusen, E.; Marculescu, B.; Cincu, C. Synthesis and Characterization of a Hybrid Material from Self-Assembling Colloidal Particles and Carbon Nanotubes. *Colloid Polym. Sci.* **2011**, *289*, 387−394.
(40) Yang, Y.-W.; Hentschel, J.; Chen, Y.-C.; Lazari, M.; Zeng, H.; Michael van Dam, R.; Guan, Z. "Clicked" Fluoropolymer Elastomers as Robust Materials for Potential Microfluidic Device Applications. *J. Mater. Chem.* **2012**, *22*, 1100−1106.
(41) Bauer, A. W.; Kirby, W. M.; Sherris, J. C.; Turck, M. Antibiotic Susceptibility Testing by a Standardized Single Disk Method. *Am. J. Clin. Pathol.* **1966**, *45*, 493−496.
(42) Lin, Q. B.; Li, B.; Song, H.; Wu, H. J. Determination of Silver in Nano-Plastic Food Packaging by Microwave Digestion Coupled with Inductively Coupled Plasma Atomic Emission Spectrometry or Inductively Coupled Plasma Mass Spectrometry. *Food Addit. Contam., Part A* **2011**, *28*, 1123−1128.
(43) Holzinger, M.; Vostrowsky, O.; Hirsch, A.; Hennrich, F.; Kappes, M.; Weiss, R.; Jellen, F. Sidewall Functionalization of Carbon Nanotubes. *Angew. Chem., Int. Ed.* **2001**, *40*, 4002−4005.
(44) Cases, M.; Duran, M.; Mestres, J.; Martín, N.; Solà, M. Mechanism of the Addition Reaction of Alkyl Azides to [60]Fullerene and the Subsequent N2 Extrusion to Form Monoimino-[60]fullerenes. *J. Org. Chem.* **2000**, *66*, 433−442.
(45) Gao, C.; He, H.; Zhou, L.; Zheng, X.; Zhang, Y. Scalable Functional Group Engineering of Carbon Nanotubes by Improved One-Step Nitrene Chemistry. *Chem. Mater.* **2008**, *21*, 360−370.
(46) Mevellec, J.-Y.; Bergeret, C.; Cousseau, J.; Buisson, J.-P.; Ewels, C. P.; Lefrant, S. Tuning the Raman Resonance Behavior of Single-Walled Carbon Nanotubes via Covalent Functionalization. *J. Am. Chem. Soc.* **2011**, *133*, 16938−16946.
(47) Yan, C. e.; Cheng, S.; Feng, L. Kinetics and Mechanism of Emulsifier-free emulsion Copolymerization: Styrene-Methyl Methacrylate-Acrylic Acid System. *J. Polym. Sci., Part A: Polym. Chem.* **1999**, *37*, 2649−2656.
(48) Wang, P. H.; Pan, C. Y. Preparation of Styrene/Acrylic Acid Copolymer Microspheres: Polymerization Mechanism and Carboxyl Group Distribution. *Colloid Polym. Sci.* **2002**, *280*, 152−159.
(49) Rusen, E.; Mocanu, A.; Marculescu, B.; Andronescu, C.; Stancu, I. C.; Butac, L. M.; Ioncea, A.; Antoniac, I., Influence of the Solid-Liquid Adhesion on the Self-Assembling Properties of Colloidal Particles. In *Photonic Crystals: Fabrication, Band Structure and Applications*, Laine, V. E., Ed.; Nova Science Publishers Inc.: New York, 2010; Chapter 9, pp 173−189.